Shorter Communication

Pergamon

Chemical Engineering Science, Vol. 50, No. 20, pp. 3313–3317, 1995

0009–2509/95 $9.50 + 0.00

0009–2509(95)00166–2

On the rapid convergence of the analytical solution of Stokes flow around spheroids-in-cell

(*First received* 5 *September* 1994; *revised manuscript received* 10 *February* 1995; *accepted* 5 *May* 1995)

1. INTRODUCTION

Analytical spheroid-in-cell flow models, designed to treat the case of transport in swarms of (prolate or oblate) spheroidal particles appeared relatively recently. Epstein and Masliyah (1972) were the first to propose a spheroid-in-cell model, but they solved the flow problem numerically, a fact that discouraged the use of that flow model for heat and mass transfer calculations. The solution of Stokes flow around a spheroidal particle immersed in a confocal spheroidal envelope of fluid, with Kuwabara-type and with Happel-type boundary conditions, was obtained in the form of a *semiseparable* expansion in Dassios *et al.* (1994) and Dassios *et al.* (1995), respectively. One of the most interesting and intriguing properties of this solution concerns the rapid convergence of the semiseparable expansion. It is shown here that the leading term of the expansion for each of the two aforementioned formulations is an excellent analytical approximation to the corresponding exact solution (obtained numerically) over a fairly broad range of the geometrical parameters. For axis ratio in the range $[\frac{1}{5}, 5]$ and solid volume fraction in the range $[0, 0.3]$, the relative error in the value of the streamfunction given by the leading term is smaller than 1%, and the relative error in the value of the friction coefficient is smaller than 2–3%. This validation of the leading term sets the ground for its use to develop simple, yet reliable, models of heat and mass transfer in swarms of spheroidal particles as in Coutelieris *et al.* (1993, 1995).

2. STOKES FLOW IN SPHEROIDAL PARTICLE-IN-CELL MODELS

Dassios *et al.* (1994) obtained the solution of axisymmetric Stokes flow in a spheroidal particle-in-cell with Kuwabara-type boundary conditions. The solid particle is a spheroid with equatorial radius $a_1 = 1$, semiaxis along the axis of symmetry equal to a_3, and semifocal length c. [All variables are in dimensionless form, unless specified otherwise, and in accordance with the notation in Dassios *et al.* (1994).] The surface of the particle is spheroidal and is specified by $\tau = \tau_\alpha = a_3/c$. The outer boundary of the unit cell is a conceptual spheroidal surface, confocal with the inner one, and is specified by $\tau = \tau_\beta = b_3/c$, where b_3 takes the value required to make the solid volume fraction of the unit cell equal to that of the swarm. The Kuwabara-type boundary conditions are as follows. On the inner boundary ($\tau = \tau_\alpha$) both velocity components, v_τ and v_ζ, vanish. On the outer boundary ($\tau = \tau_\beta$) the axial velocity component is equal to the approach velocity (unity) and the vorticity vanishes.

More recently, Dassios *et al.* (1995) obtained the solution of Stokes flow in a spheroidal particle-in-cell with Happel-type boundary conditions. According to this formulation the BCs are as follows. On the inner boundary, the two velocity components are such that the velocity vector coincides with the velocity of translation of the particle along the axis of symmetry. (The velocity of translation has magnitude equal to unity). On the outer boundary, the velocity component normal to the boundary and the shear stress vanish. This formulation has the advantage that it renders the unit cell self-sufficient in mechanical energy, as opposed to the unit-cell in the Kuwabara-type formulation.

Both of the above applications result in solutions of the form

$$\psi(\tau, \zeta) = \sum_{n=2,4,\ldots}^{\infty} g_n(\tau)\, G_n(\zeta). \tag{1}$$

The leading term of the expansion is denoted by

$$\psi^{(2)}(\tau, \zeta) = g_2(\tau)\, G_2(\zeta) \tag{2}$$

so that

$$\psi(\tau, \zeta) = \psi^{(2)}(\tau, \zeta) + \{\text{Correction Term}\} \tag{3}$$

with

$$\{\text{Correction Term}\} = \sum_{n=4,6,\ldots}^{\infty} g_n(\tau)\, G_n(\zeta). \tag{4}$$

The expression for $g_2(\tau)$ depends on the type of BCs used.

2.1. *Leading term for Happel-type BCs*

In this case

$$g_2(\tau) = \mathscr{A}_1 G_1(\tau) + C_2 G_2(\tau) + \mathscr{A}_4 G_4(\tau) + D_2 H_2(\tau) \tag{5}$$

where $\mathscr{A}_1$, C_2, $\mathscr{A}_4$ and D_2 are constant coefficients the values of which depend on the geometrical parameters τ_α and τ_β. In any particular instance, these coefficients are obtained readily by solving the linear system

$$\begin{bmatrix} G_1(\tau_\alpha) & G_2(\tau_\alpha) & G_4(\tau_\alpha) & H_2(\tau_\alpha) \\ G_1'(\tau_\alpha) & G_2'(\tau_\alpha) & G_4'(\tau_\alpha) & H_2'(\tau_\alpha) \\ G_1(\tau_\beta) & G_2(\tau_\beta) & G_4(\tau_\beta) & H_2(\tau_\beta) \\ (\tau_\beta^2 - \frac{1}{3})G_1''(\tau_\beta) & (\tau_\beta^2 - \frac{1}{3})G_2''(\tau_\beta) & (\tau_\beta^2 - \frac{1}{3})G_4''(\tau_\beta) & (\tau_\beta^2 - \frac{1}{3})H_2''(\tau_\beta) \\ -2\tau_\beta G_1'(\tau_\beta) & -2\tau_\beta G_2'(\tau_\beta) & -2\tau_\beta G_4'(\tau_\beta) & -2\tau_\beta H_2'(\tau_\beta) \end{bmatrix} \cdot \begin{bmatrix} \mathscr{A}_1 \\ C_2 \\ \mathscr{A}_4 \\ D_2 \end{bmatrix} = \begin{bmatrix} 2G_2(\tau_\alpha)/(\tau_\alpha^2 - 1) \\ 2G_1(\tau_\alpha)/(\tau_\alpha^2 - 1) \\ 0 \\ 0 \end{bmatrix} \tag{6}$$

where the primes and double-primes denote the first and second derivatives of the corresponding functions, respectively.

2.2. *Leading term for Kuwabara-type BCs*

In this case

$$g_2(\tau) = \frac{1}{D(\tau_\alpha^2 - 1)}\left[\Lambda_2 G_2(\tau) + \Lambda_3\left(\frac{5G_4(\tau_\beta)}{G_1(\tau_\beta)}G_1(\tau) + G_4(\tau)\right) + \Lambda_4 H_2(\tau)\right] \tag{7}$$

where

$$D = \frac{1}{2G_2(\tau_\beta)}[\Lambda_2 G_2(\tau_\beta) + 6\Lambda_3 G_4(\tau_\beta) + \Lambda_4 H_2(\tau_\beta)] \tag{7a}$$

and

$$\Lambda_2 = G_4(\tau_\alpha)H_2'(\tau_\alpha) - G_4'(\tau_\alpha)H_2(\tau_\alpha) - \frac{5}{\tau_\beta}G_4(\tau_\beta)[H_2(\tau_\alpha) - \tau_\alpha H_2'(\tau_\alpha)] \tag{7b}$$

$$\Lambda_3 = G_2'(\tau_\alpha)H_2(\tau_\alpha) - G_2(\tau_\alpha)H_2'(\tau_\alpha) = -\tfrac{1}{2} \tag{7c}$$

$$\Lambda_4 = G_2(\tau_\alpha)G_4'(\tau_\alpha) - G_2'(\tau_\alpha)G_4(\tau_\alpha) + \frac{5}{\tau_\beta}G_4(\tau_\beta)[G_2(\tau_\alpha) - \tau_\alpha G_2'(\tau_\alpha)]. \tag{7d}$$

Equation (7) corresponds to the original Kuwabara formulation in which the particle is stationary and the fluid flows past it with an approach velocity $\tilde{u}\hat{\mathbf{x}}_3$. The solution for the case in which the particle translates with velocity $-\tilde{u}\hat{\mathbf{x}}_3$, while the fluid has no motion other than that caused by the particle itself, is obtained by subtracting $(\tau^2 - 1)/(\tau_\alpha^2 - 1)$ from the RHS of eq. (7), taking into account that $\psi_\alpha = [(\tau^2 - 1)/(\tau_\alpha^2 - 1)]\, G_2(\zeta)$ is the expression for the stream function of the uniform flow field $\mathbf{v} = \hat{\mathbf{x}}_3$. This origin shift produces the Kuwabara formulation that corresponds to that of Happel. (Of course, the difference in the BCs on the outer envelope—vanishing vorticity vs vanishing shear stress—remains.)

2.3. *Higher-order terms*

Analytical formulae for the calculation of the higher-order terms of the expansion (1) are given in Dassios *et al.* (1994, 1995), for Kuwabara-type and Happel-type BCs, respectively. However, the manipulations become rapidly very involved, and calculation of the full correction term (beyond the first three or four terms) in this manner would not be cost effective. Below, we determine the magnitude of the correction term for various values of the geometrical parameters by comparing the "exact" solution, obtained numerically, with the leading term of the analytical solution.

3. NUMERICAL VALIDATION OF THE LEADING TERM

A numerical solution of Stokes flow in a spheroidal particle-in-cell model with both types of BCs (Happel and Kuwabara) was first reported by Epstein and Masliyah (1972). However, those results were not presented in a form that would allow us a direct comparison with the analytical results. For this reason, we developed our own numerical algorithm, using a finite difference scheme in the (τ, ζ) domain. The results obtained with this algorithm are regarded here as the "exact" solution. Of course, every test required concerning the convergence and accuracy of the numerical solution has been made, and passed.

Figure 1 shows typical streamlines around a prolate spheroid with relatively large aspect ratio, $a_3 = 5$, (which makes this case demanding) in a cell that corresponds to a sizeable solid volume fraction value, $\gamma = 0.1$. Some typical "exact" results are shown with circles, while the solid lines give the corresponding results from the leading term of the analytical solution, $\psi^{(2)}$. The agreement is very good to excellent, almost everywhere. (For a quantitative examination of the error see the discussion concerning Tables 1 and 2, below.) Some discernible discrepancy occurs only near the stagnation regions, especially for Kuwabara-type BCs. The agreement in the case of Happel-type BCs is better.

Figure 2 is similar to Fig. 1, but here the spheroidal particle is oblate, with axis ratio $a_3 = \frac{1}{2}$, and the solid volume fraction is large, $\gamma = 0.3$. The large value of γ makes this case demanding. Even so, the leading term in the case of Happel-type BCs is, again, in excellent agreement with the exact solution. The leading term in the case of Kuwabara-type BCs deviates discernibly from the exact solution, especially near the stagnation region, but it could still be useful for somewhat rough estimations.

Figure 3 gives $Re\, C_D$ as a function of the solid volume fraction γ for selected prolate and oblate spheroids, for Happel-type and Kuwabara-type BCs. The lines are obtained from the leading term, $\psi^{(2)}$, and the circles (open or full) are results from the numerical solution. The agreement is excellent over a broad range of the parameter values. The following remarks are pertinent at this point. The Reynolds number, Re, and the friction coefficient, C_D, are defined as

$$Re = \frac{2\tilde{a}_1 \tilde{\rho}\tilde{u}}{\tilde{\mu}}, \qquad C_D = \frac{\tilde{F}_D}{(\pi\tilde{a}_1^2)(\frac{1}{2}\tilde{\rho}\tilde{u}^2)} \tag{8}$$

where $\tilde{F}_D$ is the (dimensional) drag force. The drag force was obtained in closed analytical form from the leading term $\psi^{(2)}$, through a simple line integration. The "exact" results were obtained by the corresponding numerical line integration, using the numerically obtained values of ψ.

Up to this point, we have compared results obtained from the leading term of the expansion, $\psi^{(2)}$, with the "exact" results. The differences can be attributed to the correction term, eq. (3). As it turns out, the leading term contains most of the important physics and gives very good to excellent predictions, so long as the geometrical parameters remain in a moderate range, say $\frac{1}{5} \leqslant a_3 \leqslant 5$, and $0 \leqslant \gamma \leqslant 0.3$, or even

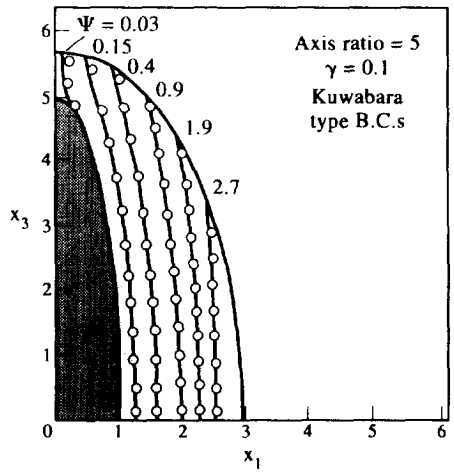

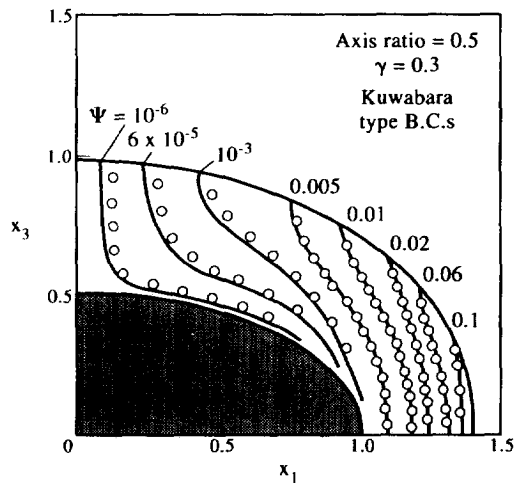

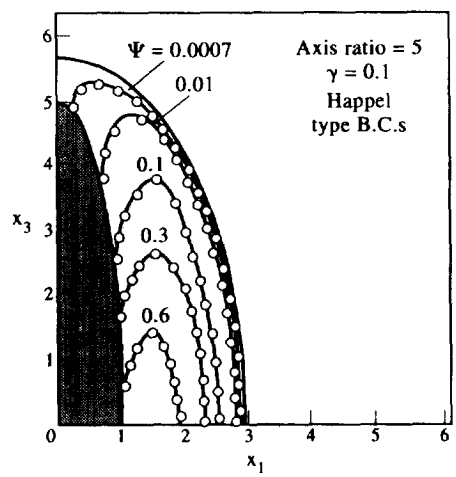

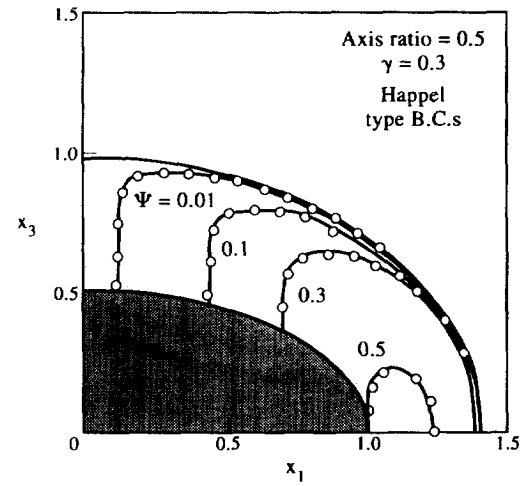

Fig. 1. Streamlines around a prolate spheroid-in-cell with axis ratio 5 and solid volume fraction 0.1, for both types of BCs. The results from the leading term of the analytical solution are shown with continuous curves, whereas those from the numerical solution are shown with small circles.

Fig. 2. Streamlines around an oblate spheroid-in-cell with axis ratio 0.5 and solid volume fraction 0.3. The results from the leading term of the analytical solution are shown with continuous curves, whereas those from the numerical solution are shown with small circles.

Table 1. Percent mean relative error in the value of the streamfunction ψ, using one ($n = 2$), two ($n = 4$) and three ($n = 6$) terms of the expansion (1)

a_3	γ	$ERR_K^{(2)}$	$ERR_K^{(4)}$	$ERR_K^{(6)}$	$ERR_H^{(2)}$	$ERR_H^{(4)}$	$ERR_H^{(6)}$
0.2	0.1	0.71	0.64	0.56	0.62	0.54	0.50
0.5	0.1	0.54	0.50	0.43	0.48	0.41	0.37
0.8	0.1	4.0×10^{-3}	2.0×10^{-3}	1.3×10^{-3}	3.3×10^{-3}	10^{-3}	8.8×10^{-4}
1.0001	0.1	1.0×10^{-14}	1.0×10^{-14}	1.0×10^{-14}	1.0×10^{-14}	1.0×10^{-14}	1.0×10^{-14}
1†	0.1	0	0	0	0	0	0
1.25	0.1	2.0×10^{-3}	1.3×10^{-3}	9.9×10^{-4}	1.1×10^{-3}	8.6×10^{-4}	6.0×10^{-4}
2.0	0.1	0.41	0.39	0.35	0.38	0.33	0.29
5.0	0.1	0.63	0.57	0.51	0.59	0.52	0.48
2.0	0.0001	5.0×10^{-5}	3.3×10^{-5}	1.6×10^{-5}	4.0×10^{-5}	3.2×10^{-5}	10^{-5}
2.0	0.001	1.0×10^{-3}	9.7×10^{-4}	8.2×10^{-4}	8.5×10^{-4}	7.6×10^{-4}	6.3×10^{-4}
2.0	0.01	0.29	0.23	0.19	0.25	0.19	0.15
2.0	0.1	0.41	0.39	0.35	0.38	0.33	0.29
2.0	0.3	0.46	0.42	0.38	0.41	0.39	0.36

Note: $ERR_J^{(n)} = 100\langle(1/\psi_J)|\psi_J - \psi_J^{(n)}|\rangle$, $n = 2, 4, 6$; $J = H, K$. ψ_J = "exact" value; $\psi_J^{(n)}$ = analytical solution at level n. $\langle\cdot\rangle$: the averaging is done over the entire grid used in the numerical solution.

†For $a_3 = 1$, the leading term is the exact solution.

Table 2. Percent mean relative error in the value of the $Re\,C_D$, using one ($n = 2$), two ($n = 4$) and three ($n = 6$) terms of the expansion (1)

a_3	γ	$ERR_K^{(2)}$	$ERR_K^{(4)}$	$ERR_K^{(6)}$	$ERR_H^{(2)}$	$ERR_H^{(4)}$	$ERR_H^{(6)}$
0.2	0.1	2.09	1.87	1.75	1.96	1.84	1.71
0.5	0.1	1.32	1.25	1.17	1.17	1.13	0.98
0.8	0.1	0.41	0.36	0.31	0.34	0.27	0.19
1.0001	0.1	2.0×10^{-10}	2.0×10^{-10}	2.0×10^{-10}	1.9×10^{-10}	1.9×10^{-10}	1.9×10^{-10}
1†	0.1	0	0	0	0	0	0
1.25	0.1	0.32	0.29	0.24	0.28	0.21	0.15
2.0	0.1	1.11	0.95	0.88	1.06	0.92	0.83
5.0	0.1	1.95	1.83	1.72	1.89	1.81	1.68
2.0	0.0001	0.78	0.72	0.65	0.74	0.69	0.60
2.0	0.001	0.97	0.83	0.77	0.94	0.81	0.73
2.0	0.01	1.05	0.92	0.84	1.01	0.89	0.81
2.0	0.1	1.11	0.95	0.88	1.06	0.92	0.83
2.0	0.3	1.23	1.15	1.05	1.19	1.12	1.02

Note: $ERR_J^{(n)} = 100\langle[1/(Re\,C_D)_J]|(Re\,C_D)_J - (Re\,C_D)_J^{(n)}|\rangle$, $n = 2,4,6$; $J = H,K$. $(Re\,C_D)_J$ = "exact" value; $(Re\,C_D)_J^{(n)}$ = analytical solution at level n. $\langle\cdot\rangle$: the averaging is done over the entire grid used in the numerical solution.

†For $a_3 = 1$, the leading term is the exact solution.

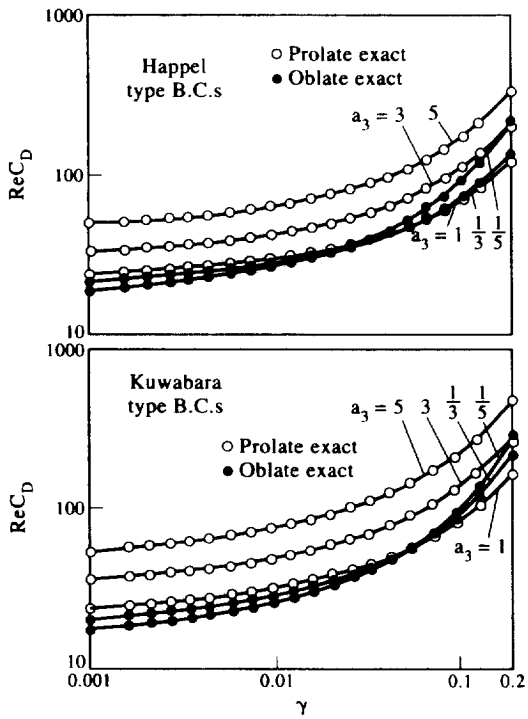

Fig. 3. Plot of $Re\,C_D$ vs the solid volume fraction γ, for selected prolate ($a_3 > 1$) and oblate ($a_3 < 1$) spheroid-in-cell geometries, for both types of BC formulation. The results from the leading term are shown with lines, whereas those from the numerical "exact" solution are shown with small circles (open or full).

beyond this range if a rougher approximation is satisfactory. This is attributed to the fact that the leading term satisfies all the BCs exactly, while it satisfies the differential equation, eq. (1), approximately. All the rest of the expansion (namely, the correction term) is needed to make the small adjustment necessary for $E^4\psi = 0$ to be satisfied exactly. Having reached this conclusion, it is important to examine whether the individual terms of the expansion that comprises the correction term form a rapidly diminishing sequence, or whether (conceivably) the higher-order terms are sizeable and they simply happen to have a small sum through cancellation. The results of Tables 1 and 2 show that, fortunately, the former is the case.

Table 1 gives the percent mean relative error in the value of the streamfunction ψ, when one uses the leading term only ($ERR_H^{(2)}$, $ERR_K^{(2)}$), when one uses the first two terms ($ERR_H^{(4)}$, $ERR_K^{(4)}$), and when one uses the first three terms ($ERR_H^{(6)}$, $ERR_K^{(6)}$) of the expansion. The subscripts H and K indicate Happel-type and Kuwabara-type BCs, respectively. We observe the following.

- The mean relative error in ψ is very small (of the order of 1% or less) over the range $\{\frac{1}{5} \leqslant a_3 \leqslant 5, 0 \leqslant \gamma \leqslant 0.3\}$.
- The mean relative error in ψ increases as the deviation of the axis ratio, a_3, from unity (for $a_3 = 1$ the leading term $\psi^{(2)}$ is the *exact* solution) increases and as the solid volume fraction, γ, increases.
- The second and third terms, each, provide small corrections, and they do not show sign alternation.
- The relative error for Happel-type BCs is smaller than that for Kuwabara-type BCs.

Table 2 gives the percent mean relative error in the value of $Re\,C_D$, when one uses the leading term only, when one uses the first two terms, and when one uses the first three terms of the expansion. We observe the following.

- The mean relative error in $Re\,C_D$ is small (of the order of 2–3% or less) over the range $\{\frac{1}{5} \leqslant a_3 \leqslant 5, 0 \leqslant \gamma \leqslant 0.3\}$.
- The mean relative error in $Re\,C_D$ increases as the deviation of the axis ratio, a_3, from unity (for $a_3 = 1$ the leading term gives the exact solution) increases and as the solid volume fraction, γ, increases.
- The second and third terms, each, provide small corrections, and they do not show sign alternation.
- The relative error for Happel-type BCs is smaller than that for Kuwabara-type BCs.

4. CONCLUSIONS

Evaluation of the validity of the leading term $\psi^{(2)}(\tau,\zeta)$ in the expansion (1) was made through comparison with the exact solution, obtained numerically, in the case of a flow problem of considerable practical interest. The problem under consideration is that of Stokes flow around a spheroidal particle in a spheroidal envelope, the solution of which in the

form of eq. (3) was obtained recently, with Kuwabara-type BCs (Dassios *et al.* 1994), and Happel-type BCs (Dassios *et al.*, 1995). For axis ratio $a_3 = 1$, the leading term coincides with the exact solution for spherical geometry. As a_3 deviates from unity ($a_3 > 1$ for prolate spheroids, $a_3 < 1$ for oblate spheroids), the discrepancy between the leading term and the exact solution becomes discernible, but it remains small for moderate values of a_3. In the range $\{\frac{1}{5} \leqslant a_3 \leqslant 5, 0 \leqslant \gamma \leqslant 0.3\}$ the leading term is an excellent approximation to the exact solution; the relative error in ψ given by the leading term in this range remains smaller than $\sim 1\%$, while the relative error in the friction coefficient remains smaller than 2–3%. Hence, the leading term $\psi^{(2)}$ can be used for most engineering applications in this range, and even beyond, if rougher approximations are acceptable.

This remarkably good behavior of the leading term is attributed to the fact that it satisfies exactly all the BCs (in both types of formulation), and at the same time it is a very good *approximate* solution of the differential equation $E^4\psi = 0$. All the rest of the expansion is needed to make the small correction that is required for the above equation to be satisfied exactly. The magnitudes of the individual terms of the rest of the expansion are small compared to the leading term, and form a rapidly diminishing sequence.

Acknowledgements—This work was supported by the Institute of Chemical Engineering and High Temperature Chemical Processes (ICE/HT-FORTH).

V. N. BURGANOS
F. A. COUTELIERIS
G. DASSIOS
A. C. PAYATAKES†

†Corresponding author.

Institute of Chemical Engineering
and High Temperature Chemical Processes, and
Department of Chemical Engineering
University of Patras
GR 265 00 Patras, Greece

REFERENCES

Coutelieris, F. A., Burganos, V. N. and Payatakes, A. C., 1993, On mass transfer from a Newtonian fluid to a swarm of adsorbing spheroidal particles for high Peclet numbers. *J. Colloid Interface Sci.* **161**, 43–52.

Coutelieris, F. A., Burganos, V. N. and Payatakes, A. C., 1995, Convection diffusion and adsorption in a swarm of spheroidal particles. *A.I.Ch.E. J.* (in press).

Dassios, G., Hadjinicolaou, M. and Payatakes, A. C., 1994, Generalized eigenfunctions and complete semiseparable solutions for Stokes flow in spheroidal coordinates. *Q. Appl. Math.* **52**, 157–191.

Dassios, G., Hadjinicolaou, M., Coutelieris, F. A. and Payatakes, A. C., 1995, Stokes flow in spheroidal particle-in-cell models with Happel and Kuwabara boundary conditions. *Int. J. Engng Sci.* **33**, 1465–90.

Epstein, N. and Masliyah, J. H., 1972, Creeping flow through clusters of spheroids and elliptical cylinders. *Chem. Engng J.* **3**, 169–175.